Integrated Aerodynamic-Structural Design of a Transport Wing

B. Grossman,* R. T. Haftka,† P.-J. Kao,‡ D. M. Polen,§ and M. Rais-Rohani¶
Virginia Polytechnic Institute and State University, Blacksburg, Virginia 24061
and
J. Sobieszczanski-Sobieski**
NASA Langley Research Center, Hampton, Virginia 23665

The integrated aerodynamic-structural design of a subsonic transport wing for minimum weight subject to required range is formulated and solved. The problem requires large computational resources, and two methods are used to alleviate the computational burden. First, a modular sensitivity method that permits the usage of black-box disciplinary software packages is used to reduce the cost of sensitivity derivatives. In particular, it is shown that derivatives of the aeroelastic response and divergence speed can be calculated without the costly computation of derivatives of aerodynamic influence coefficient and structural stiffness matrices. A sequential approximate optimization is used to further reduce computational cost. The optimization procedure is shown to require a relatively small number of analysis and sensitivity calculations.

Introduction

AIRCRAFT design requires the integration of several disciplines, including aerodynamics, structures, controls, and propulsion. Traditionally, the design process would proceed sequentially with feedback limited to the conceptual design level. In the last few years, there has been more interest in integrating the design procedure. This was motivated by the introduction of composite materials that tend to create stronger aeroelastic interactions, as well as by the requirements of advanced vehicles, such as the aerospace plane, where, because of extreme flight conditions, the interdisciplinary interactions are particularly important.

One of the more important interdisciplinary interactions in modern aircraft design is that of aerodynamics and structures. One aspect of that interaction is the use of composite materials to tailor the deformation of aircraft wings so as to affect aerodynamic loads. This so-called aeroelastic tailoring is the focus of many publications (see Refs. 1 and 2 for recent reviews of the state-of-the-art). Aeroelastic tailoring is particularly important for forward-swept-wing aircraft, such as the Grumman X-29A, because of the aeroelastic instabilities that tend to plague forward-swept wings.

Aeroelastic tailoring is a limited form of integrated design, as the structure is designed to affect aerodynamic properties, but the aerodynamic design does not consider structural constraints, except in a very broad sense (such as in limits on wing aspect ratio and thickness). In Ref. 3, it has been shown that in an integrated design process, it is reasonable to use a suboptimal aerodynamic design if it results in reduced structural weight, because the weight savings can be converted into improved aerodynamic efficiency.

There have been several papers on integrated aerodynamic-structural design of aircraft wings in recent years. Some focus on the use of multilevel techniques to coordinate the overall design of the airplane with the aerodynamic and structural designs, e.g., Refs. 4 and 5. Others focus on more complex interactions such as the inclusion of active controls, e.g., Ref. 6. The present paper is focused on the computational aspects of the design process.

The computational cost associated with integrated aerodynamic-structural design is a formidable obstacle to its implementation for most practical wing design problems. This alone can strain the capabilities of today's supercomputers. Ref. 7 considered several techniques for improving computational efficiency of integrated aerodynamic-structural wing design using a sailplane wing example. This paper continues the work of Ref. 7 for a forward-swept, transport wing. This transport wing was also studied in Ref. 8, where the wing structure was optimized for a fixed aerodynamic design.

For practical wing design problems the major components of the cost of the design optimization are the analysis and sensitivity computations. The cost of the optimization operations is small in comparison. Therefore, this paper is focused on reducing the cost of sensitivity calculations and reducing the number of required analysis by employing a sequential approximate optimization technique. A recently developed technique for modular sensitivity analysis [also known as the Global Sensitivity Equation (GSE) technique[9,10]] is used to obtain efficiently cross-disciplinary sensitivities such as devivatives of structural deformations with respect to changes in aerodynamic shape. This method also permits the use of black-box disciplinary programs, and so is very useful in the integration of structural and aerodynamic software packages. In particular, it is shown that it is possible to calculate derivatives of aeroelastic quantities such as divergence speed without the need for obtaining derivatives of aerodynamic influence coefficient matrices.

Aeroelastic Formulation

The aeroelastic analysis of the wing is simplified by making several assumptions. We assume that the effect of the aerodynamics on structural deformations can be approximated by lumping the aerodynamic forces at n_l structural grid points (called here the load set) and including only the vertical

Presented as Paper 89-2129 at the AIAA/AHS/ASEE Aircraft Design Systems, and Operations Conference, Seattle, WA, July 31–Aug. 2, 1989; received Oct. 11, 1989; revision received March 15, 1990; accepted for publication April 18, 1990.

Authors listed alphabetically.

*Professor, Department of Aerospace and Ocean Engineering. Associate Fellow AIAA.

†Christopher C. Kraft Professor, Department of Aerospace and Ocean Engineering. Member AIAA.

‡Graduate Student, Department of Aerospace and Ocean Engineering; currently Research Scientist, Analytical Services and Materials, Inc., Hampton, VA. Member AIAA.

§Graduate Student, Department of Aerospace and Ocean Engineering; currently Associate Engineer, Atlantic Research Corp., Gainesville, VA.

¶Graduate Student, Department of Aerospace and Ocean Engineering.

**Head, Interdisciplinary Research Office. Associate Fellow AIAA.

components of the loads. The vector of vertical aerodynamic loads is denoted as $\boldsymbol{F}_a$. We assume that the overall aircraft response affects the wing only through the root angle of attack α. Finally, we assume that the effect of structural deformations on the aerodynamic response can be approximated in terms of the vector of vertical displacements $\boldsymbol{\theta}$ at the load set.

The vertical aerodynamic loads at the load set $\boldsymbol{F}_a$ are determined from an aerodynamic analysis procedure. For low-speed wing designs, we utilize a vortex lattice method (e.g., Ref. 11) to compute the lift and induced drag. The wing is discretized into panels, with each panel containing an element of a horseshoe vortex of strength γ_j. By enforcing flow tangency at each panel, a vector of circulation strengths $\boldsymbol{\Gamma}$ may be computed from

$$V(\boldsymbol{p},\boldsymbol{\theta})\boldsymbol{\Gamma} = \boldsymbol{C}(\boldsymbol{p},\alpha,\boldsymbol{\theta}) \tag{1}$$

where $\boldsymbol{p}$ is a vector of design parameters and V a matrix of influence coefficients. The aerodynamic forces are computed from a local application of the Kutta-Joukowski theorem, and compressibility effects are included through a Göthert transformation. The profile drag for each wing section is calculated from the measured airfoil drag polar. The load vector $\boldsymbol{F}_a$ is then obtained as

$$\boldsymbol{F}_a = \boldsymbol{F}_a(\boldsymbol{p},\alpha,\boldsymbol{\theta},\boldsymbol{\Gamma}) \tag{2}$$

Altogether we combine Eqs. (1) and (2) as

$$\boldsymbol{F}_a = \boldsymbol{f}_1(\boldsymbol{p},\alpha,\boldsymbol{\theta}) \tag{3}$$

The angle of attack is obtained from the overall vertical equilibrium of the aircraft as

$$f_2(\boldsymbol{p},\boldsymbol{F}_a) = ½nW - N^T\boldsymbol{F}_a = 0 \tag{4}$$

where N is a summation vector, n the load factor, and W the weight of the aircraft.

The vertical displacements at the load set are calculated by finite element analysis using a modification of the WIDOWAC[12] program. First, the nodal displacement vector $\boldsymbol{U}$ is calculated by solving

$$K(\boldsymbol{p})\boldsymbol{U} = T\boldsymbol{F}_a + n\boldsymbol{F}_I(\boldsymbol{p}) \tag{5}$$

where K is the stiffness matrix, T a Boolean matrix that expands $\boldsymbol{F}_a$ to the full set of structural degrees of freedom, and $\boldsymbol{F}_I$ the gravitational and inertia load vector. Strains and stresses are then calculated from the displacement vector $\boldsymbol{U}$. The vertical displacements at the load set $\boldsymbol{\theta}$ are extracted from $\boldsymbol{U}$ as

$$\boldsymbol{\theta} = T^T\boldsymbol{U} \tag{6}$$

Equations (5) and (6) can be combined as

$$\boldsymbol{\theta} = \boldsymbol{f}_3(\boldsymbol{p},\boldsymbol{F}_a) \tag{7}$$

Solution Procedure

Equations (3), (4), and (7) are a set of nonlinear coupled equations for the vector of vertical aerodynamic loads $\boldsymbol{F}_a$, the wing root angle of attack α, and the vector of vertical displacements $\boldsymbol{\theta}$. For the analysis problem, the vector of design parameters $\boldsymbol{p}$ is given. References 9 and 10 presented a modular sensitivity analysis of such coupled interdisciplinary equations. The modular approach permits treating the individual discipline analysis procedures as black boxes that do not need to be changed in the integration procedure. Here, we employ a similar approach for the sensitivity analysis, with $\boldsymbol{f}_1$ representing an aerodynamic black box and $\boldsymbol{f}_3$ a structural black box. We also use the same approach for the solution of the system via Newton's method.

Given an initial estimate for the solution $\boldsymbol{F}_a^0,\alpha^0,\boldsymbol{\theta}^0$, we use Newton's method to improve that estimate. The iterative process may be written as

$$J\,\Delta\boldsymbol{Y} = \Delta\boldsymbol{f} \tag{8}$$

where

$$\Delta\boldsymbol{Y} = \begin{Bmatrix} \Delta\boldsymbol{F}_a \\ \Delta\alpha \\ \Delta\boldsymbol{\theta} \end{Bmatrix} \tag{9}$$

and

$$\Delta\boldsymbol{f} = \begin{Bmatrix} \boldsymbol{f}_1(\boldsymbol{p},\alpha^0,\boldsymbol{\theta}^0) - \boldsymbol{F}_a^0 \\ f_2(\boldsymbol{p},\boldsymbol{F}_a^0) \\ \boldsymbol{f}_3(\boldsymbol{p},\boldsymbol{F}_a^0) - \boldsymbol{\theta}^0 \end{Bmatrix} \tag{10}$$

and the Jacobian J is given as

$$J = \begin{bmatrix} I & -\partial\boldsymbol{f}_1/\partial\alpha & -\partial\boldsymbol{f}_1/\partial\boldsymbol{\theta} \\ -\partial f_2/\partial\boldsymbol{F}_a & 0 & 0 \\ -\partial\boldsymbol{f}_3/\partial\boldsymbol{F}_a & 0 & I \end{bmatrix}$$

$$= \begin{bmatrix} I & -q\boldsymbol{R} & -qA \\ N^T & 0 & 0 \\ -S & 0 & I \end{bmatrix} \tag{11}$$

The Jacobian is given in terms of the dynamic pressure q, the incremental aerodynamic force vector $q\boldsymbol{R}$, the aerodynamic influence coefficient matrix qA, and the flexibility matrix S. The incremental aerodynamic force is defined such that its component qr_i represents the change in F_{ai} due to a unit change in α, and the aerodynamic influence coefficient matrix is defined such that its component qa_{ij} represents the change in F_{ai} due to unit change in θ_j. Similarly, the flexibility matrix is such that s_{ij} is the change in θ_i due to a unit change in F_{aj}.

Partial solution of Eq. (8) yields the following three equations for the increments $\Delta\boldsymbol{\theta}$, $\Delta\alpha$ and $\Delta\boldsymbol{F}_a$:

$$(I - qSA^x)\,\Delta\boldsymbol{\theta} = SB\,\Delta\boldsymbol{f}_1 + (S\boldsymbol{R}/N^T\boldsymbol{R})\,\Delta f_2 + \Delta\boldsymbol{f}_3 \tag{12}$$

$$\Delta\alpha = (\Delta f_2 - N^T\,\Delta\boldsymbol{f}_1 - qN^TA\,\Delta\boldsymbol{\theta})/qN^T\boldsymbol{R} \tag{13}$$

$$\Delta\boldsymbol{F}_a = \Delta\boldsymbol{f}_1 + q\boldsymbol{R}\,\Delta\alpha + qA\,\Delta\boldsymbol{\theta} \tag{14}$$

Now we define

$$B \equiv I - (\boldsymbol{R}N^T)/(N^T\boldsymbol{R}) \tag{15}$$

$$A^x \equiv BA \tag{16}$$

In our case, we start with a rigid wing approximation $\boldsymbol{F}_a^0 = \boldsymbol{F}_{ar}$, $\alpha^0 = \alpha_r$, $\boldsymbol{\theta}^0 = 0$, where

$$\boldsymbol{F}_{ar} = \boldsymbol{f}_1(\boldsymbol{p},0,0) + q\alpha_r\boldsymbol{R} \tag{17}$$

$$\alpha_r = [½nW - N^T\boldsymbol{f}_1(\boldsymbol{p},0,0)]/qN^T\boldsymbol{R} \tag{18}$$

and execute a single Newton iteration to approximate the flexible wing response.

The aeroelastic divergence instability is calculated at a fixed angle of attack because it is assumed that the pilot does not react fast enough to change the angle of attack as the wing diverges. The instability is characterized by a homogeneous solution to Eq. (8), that is

$$\begin{bmatrix} I & -qA \\ -S & I \end{bmatrix} \begin{Bmatrix} \Delta \boldsymbol{F}_a \\ \Delta \boldsymbol{\theta} \end{Bmatrix} = 0 \tag{19}$$

Equation (19) is an eigenvalue problem for q. The lowest eigenvalue is the divergence dynamic pressure q_D. We denote the corresponding eigenvector as $[\boldsymbol{F}_{aD}, \boldsymbol{\theta}_D]^T$. Equation (19) can be reduced to a standard linear eigenproblem by substituting for $\Delta\boldsymbol{\theta}$ in terms of $\Delta \boldsymbol{F}_a$ to obtain

$$[AS - (1/q)I]\,\Delta \boldsymbol{F}_a = 0 \tag{20}$$

In the present aeroelastic divergence analysis, only the wing is modeled, neglecting the effect of interaction with the fuselage. This effect may be of consequence for forward-swept wings.[13,14]

Sensitivity Calculation

As stated, it is common practice to follow the preceding procedure and use a single Newton's iteration in the analysis of a flexible wing. Then for a design problem, where derivatives with respect to a design parameter p are required, Eqs. (12–14) are differentiated with respect to p (e.g., Ref. 7). This approach requires the calculation of derivatives of the matrices A and S, which can be very costly. Here, instead, we follow Refs. 9 and 10 and differentiate Eqs. (3), (4), and (7) with respect to p to obtain

$$JY' = f' \tag{21}$$

where a prime denotes differentiation with respect to p and where

$$Y' = [\boldsymbol{F}'_a\, \alpha'\, \boldsymbol{\theta}']^T \tag{22}$$

$$f' = [f'_1 f'_2 f'_3]^T \tag{23}$$

along with the definition $f'_i = \partial f_i/\partial p$ for $i = 1,2,3$. The Jacobian J appearing in Eq. (21) is the identical matrix utilized in the analysis in Eq. (11). Equation (21) can be partially solved to yield

$$(I - qSA^x)\boldsymbol{\theta}' = SBf'_1 + (S\boldsymbol{R}/N^T\boldsymbol{R})f'_2 + f'_3 \tag{24}$$

$$\alpha' = (f'_2 - N^T f'_1 - qN^T A\boldsymbol{\theta}')/qN^T\boldsymbol{R} \tag{25}$$

$$\boldsymbol{F}'_a = f'_1 + q\boldsymbol{R}\alpha' + qA\boldsymbol{\theta}' \tag{26}$$

This approach does not require any derivatives of A and S but only partial derivatives of f_1, f_2, and f_3. For example, f'_1 denotes the derivative of $\boldsymbol{F}_a$ with respect to a design variable when α and $\boldsymbol{\theta}$ are fixed.

By contrast, the more traditional approach (e.g., Ref. 7) to the derivative calculation is obtained by differentiating the aeroelastic analysis equations, such as Eqs. (12–14) with respect to p. For example, consider the derivative of Eq. (12) with respect to p

$$\begin{aligned}(I - qSA^x)\,\Delta\boldsymbol{\theta}' &= qS'A^x\,\Delta\boldsymbol{\theta} + qSBA'\,\Delta\boldsymbol{\theta} + qSB'A\,\Delta\boldsymbol{\theta} \\ &+ S'B\,\Delta f_1 + SB'\,\Delta f_1 + SB\,\Delta f'_1 + (S'\boldsymbol{R}/N^T\boldsymbol{R})\,\Delta f_2 \\ &+ S(\boldsymbol{R}/N^T\boldsymbol{R})'\,\Delta f_2 + (S\boldsymbol{R}/N^T\boldsymbol{R})\,\Delta f'_2 + \Delta f'_3 \end{aligned} \tag{27}$$

This complicated expression can be shown to be equivalent to Eq. (24). However, the traditional approach that employs Eq. (27) requires the expensive calculation of the derivatives of the aerodynamic influence coefficient matrix A' and the derivatives of the flexibility matrix S'.

Note that Eqs. (24–26) are based on the Jacobian J being calculated at the point where Eqs. (3), (4), and (7) are satisfied. Because the single Newton iteration satisfies these equations only approximately, the derivatives are also approximate. Furthermore, the derivatives of the approximations to $\boldsymbol{F}_a$, α, $\boldsymbol{\theta}$ are not precisely equal to approximate derivatives of these quantities. (Our experience indicates reasonable agreement between the two.)

To find the derivative of the divergence dynamic pressure q_D with respect to a design parameter p, we differentiate Eq. (19) at $q = q_D$ with respect to p

$$\begin{bmatrix} I & -q_D A \\ -S & I \end{bmatrix} \begin{Bmatrix} \boldsymbol{F}'_{aD} \\ \boldsymbol{\theta}'_D \end{Bmatrix} + \begin{bmatrix} 0 & -(q_D A)' \\ -S' & 0 \end{bmatrix} \begin{Bmatrix} \boldsymbol{F}_{aD} \\ \boldsymbol{\theta}_D \end{Bmatrix} = 0 \tag{28}$$

We premultiply Eq. (28) by the left eigenvector of Eq. (19) $[\boldsymbol{F}^T_{aL}, \boldsymbol{\theta}^T_L]$ defined by

$$[\boldsymbol{F}^T_{aL}, \boldsymbol{\theta}^T_L] \begin{bmatrix} I & -q_D A \\ -S & I \end{bmatrix} = 0 \tag{29}$$

and obtain

$$[\boldsymbol{F}^T_{aL}, \boldsymbol{\theta}^T_L] \begin{bmatrix} 0 & -(q_D A)' \\ -S' & 0 \end{bmatrix} \begin{Bmatrix} \boldsymbol{F}_{aD} \\ \boldsymbol{\theta}_D \end{Bmatrix} = 0 \tag{30}$$

or

$$q'_D = -\frac{q_D \boldsymbol{F}^T_{aL} A' \boldsymbol{\theta}_D + \boldsymbol{\theta}^T_L S' \boldsymbol{F}_{aD}}{\boldsymbol{F}^T_{aL} A \boldsymbol{\theta}_D} \tag{31}$$

Equation (31) contains derivatives of A and S with respect to p, which we have managed to avoid before. However, the corresponding terms can be simplified. Using the definition of S, Eq. (11), we note that

$$S'\boldsymbol{F}_{aD} = \frac{\partial}{\partial p}\left(\frac{\partial f_3}{\partial \boldsymbol{F}_a}\right)\boldsymbol{F}_{aD} \tag{32}$$

To see how $S'\boldsymbol{F}_{aD}$ can be calculated without obtaining S', consider a more generic case. Let f be a function of a vector $\boldsymbol{X}$ and let $\boldsymbol{D}$ be a given unit vector. Let $\boldsymbol{X}_0$ be a particular choice for $\boldsymbol{X}$, then the scalar product of the gradient $\partial f/\partial \boldsymbol{X}$ at $\boldsymbol{X}_0$ and the vector $\boldsymbol{D}$ is the directional derivative of f in the direction $\boldsymbol{D}$, that is

$$\begin{aligned}\left.\frac{\partial f}{\partial \boldsymbol{X}}\right|_{X_0} \boldsymbol{D} &= \lim_{\varepsilon\to 0} \frac{1}{\varepsilon}[f(\boldsymbol{X}_0 + \varepsilon \boldsymbol{D}) - f(\boldsymbol{X}_0)] \\ &= \frac{\mathrm{d}}{\mathrm{d}\varepsilon}[f(\boldsymbol{X}_0 + \varepsilon \boldsymbol{D})]_{\varepsilon=0}\end{aligned} \tag{33}$$

It is easy to check that Eq. (33) holds if $\boldsymbol{D}$ is not a unit vector, but has arbitrary magnitude. Equation (33) provides us with a way of calculating the product $\partial f/\partial X$ times D without calculating the individual components of $\partial f/\partial X$. If we now consider Eq. (32) and use $\boldsymbol{F}_a$ as the vector $\boldsymbol{X}$ and $\boldsymbol{F}_{aD}$ as the vector $\boldsymbol{D}$ we can write for each component f_{3_i} of f_3

$$\left(\frac{\partial f_{3_i}}{\partial \boldsymbol{F}_a}\right)\boldsymbol{F}_{aD} = \frac{\mathrm{d}}{\mathrm{d}\varepsilon}[f_{3_i}(\boldsymbol{F}_{a0} + \varepsilon \boldsymbol{F}_{aD})]_{\varepsilon=0} \tag{34}$$

where $\boldsymbol{F}_{a0}$ is the nominal value of $\boldsymbol{F}_a$, and the index i varies from 1 to n_l. Note that $\partial f_{3_i}/\partial \boldsymbol{F}_a$ is a row vector with elements composed of the derivatives of f_{3_i}, with respect to the individual components of $\boldsymbol{F}_a$. Equation (34) can also be written as

$$\left(\frac{\partial f_3}{\partial \boldsymbol{F}_a}\right)\boldsymbol{F}_{aD} = \frac{\mathrm{d}}{\mathrm{d}\epsilon}[f_3(\boldsymbol{F}_{a0} + \epsilon \boldsymbol{F}_{aD})]_{\epsilon=0} \tag{35}$$

where $\partial f_3/\partial \boldsymbol{F}_a$ is a matrix whose ith row is $\partial f_{3_i}/\partial \boldsymbol{F}_a$, so that it is the structural flexibility matrix S, see Eq. (11). From Eqs.

(5–7), we see that f_3 is a linear function of $\boldsymbol{F}_a$, and therefore, to calculate the right side of Eq. (35) we solve

$$KU_D = TF_{aD} \tag{36}$$

$$\frac{\mathrm{d}}{\mathrm{d}\varepsilon}[f_3(\boldsymbol{F}_{a0} + \varepsilon \boldsymbol{F}_{aD})]_{\varepsilon=0} = T^T U_D \tag{37}$$

For Eq. (32), we need to calculate the derivative of $(\partial f_3/\partial \boldsymbol{F}_a)\boldsymbol{F}_{aD}$ with respect to $\boldsymbol{p}$, [keeping $\boldsymbol{F}_{aD}$ fixed, because the derivative with respect to $\boldsymbol{p}$ in Eq. (32) applies only to the flexibility matrix S]. This can be done analytically or by finite differences.

Considering computational effort, we note that to obtain S' we need derivatives of n_l solutions to the structural equations (as S' is calculated by imposing n_l unit loads). The proposed process requires only the derivative of a single displacement solution, Eqs. (36) and (37). It is easy to verify that the solution of Eqs. (36) and (37) is $\boldsymbol{\theta}_D$. However the derivative of that solution with respect to $\boldsymbol{p}$ is not $\boldsymbol{\theta}'_D$ because $\boldsymbol{F}_{aD}$ is kept constant.

To calculate the term $A'\boldsymbol{\theta}_D$ we go through a similar process, noting that

$$qA'\boldsymbol{\theta}_D = \frac{\partial}{\partial \boldsymbol{p}}\left(\frac{\partial f_1}{\partial \boldsymbol{\theta}}\right)\boldsymbol{\theta}_D \tag{38}$$

$$\frac{\partial f_1}{\partial \boldsymbol{\theta}}\boldsymbol{\theta}_D = \frac{\mathrm{d}}{\mathrm{d}\varepsilon}[f_1(\boldsymbol{\theta}_0 + \varepsilon\boldsymbol{\theta}_D)]_{\varepsilon=0} \tag{39}$$

where $\boldsymbol{\theta}_0$ is the nominal value for $\boldsymbol{\theta}$. This time f_1 is not a linear function of $\boldsymbol{\theta}$, so that the right side of Eq. (39) needs to be calculated by finite differences or analytically from Eqs. (1) and (2). The derivative of this quantity with respect to $\boldsymbol{p}$ is again calculated by finite-differences or by analytical differentiation of the right side of Eq. (39). Again, we do not need to use Eq. (39) for the nominal $\boldsymbol{p}$ because, as can be seen from Eq. (19), with $\Delta \boldsymbol{F}_a = \boldsymbol{F}_{aD}$, $\Delta\boldsymbol{\theta} = \boldsymbol{\theta}_D$, for the nominal design, $(\partial f_1/\partial\boldsymbol{\theta})\boldsymbol{\theta}_D$ is $\boldsymbol{F}_{aD}$. The computational effort is associated with the solution of the aerodynamic problem for shape perturbation $\varepsilon\boldsymbol{\theta}_D$ for $\boldsymbol{p} + \Delta\boldsymbol{p}$. By contrast, the calculation of A' requires the perturbation of n_l aerodynamic solutions.

Forward-Swept-Wing Design Problem

We consider the design of a forward-swept wing for a subsonic transport aircraft. The design of the wing is formulated so as to reduce the weight on the aircraft while maintaining a given range. This design problem, while focusing on the wing, depends on the properties of the rest of the aircraft. For the present study, a transonic transport design, obtained in a recent design study at NASA Langley Research Center was used as a reference airplane, and its pertinent characteristics are given in Table 1. Currently, the computational costs associated with transonic aerodynamics in numerical optimization is prohibitive. As a first step, the aft-swept wing of the reference aircraft is replaced with a forward-swept wing, and the cruise Mach number is reduced from 0.78 to 0.48. Future work will endeavor to find additional computational savings in order to consider transonic aerodynamics in integrated design. The reduction to a subcritical Mach number can be expected to reduce the weight of the transport because of the reduced drag associated with the lower flight speed.

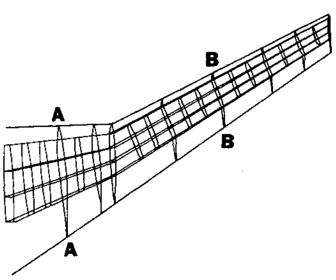

Fig. 1 Finite element model of wing structure.

Table 1 Reference aircraft specifications

Weight, N:	
W_{gw}	4.494×10^5
W_{rs}	2.852×10^5
W_{uf}	2.738×10^4
W_p	1.368×10^5
W_{rw}	3.020×10^4
Wing:	
Aspect ratio	14
Area, m^2	83.98
Span, m	34.29
Thickness, %	12
Sweep, deg	15
Taper ratio	0.25
Average cruise:	
Mach number	0.78
C_L	0.672
L/D	20.7
Specific fuel consumption	0.430
Range, m:	2.34×10^6

Table 2 Design variables

8 Geometric design variables:	29 Structural design variables:
Root chord	Panel thicknesses (11–34)
Break chord	Spar-cap areas (35–38)
Tip chord	Ply orientation (39)
Root to break	
Break to tip	
Sweep angle	
Twist angle at break	
Twist angle at tip	
2 Performance design variables:	
Cruise dynamic pressure	
Usable fuel weight	

Table 3 Design constraints

305 Structural constraints:
Maximum skin strain (1–228)
Maximum spar-cap stress (229–304)
Divergence dynamic pressure (305)
2 Performance constraints:
Range
Fuel volume

The objective function to be minimized is the gross weight of the aircraft W given as

$$W = W_s + W_{uf} + W_p \tag{40}$$

where W_s is the aircraft standard empty weight, W_{uf} is the usable fuel weight, and W_p the payload weight. The payload weight is taken to be the same as for the reference aircraft, and the usable fuel weight is a design variable adjusted by the optimization procedure so as to satisfy the range requirement. The standard empty weight of the aircraft W_s is calculated from the standard empty weight of the reference aircraft W_{rs} by assuming that structural weight savings in the wing are amplified by a factor η due to corresponding savings in nonstructural weight and in the tail and fuselage. That is

$$W_s = W_{rs} - \eta(W_{rw} - W_w) \tag{41}$$

where W_{rw} and W_w are the structural weight of the wings of the reference and design aircraft, respectively. In the present study, η is assumed to be 2.

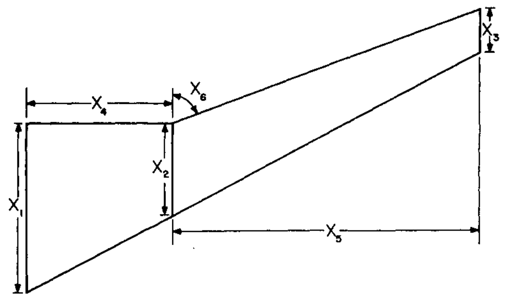

Fig. 2 Planform design variables.

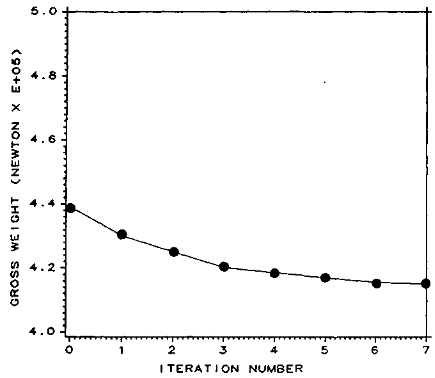

Fig. 3 Gross weight—convergence history.

Table 4 Comparison of CPU times for aeroelastic sensitivities (CPU seconds on IBM 3090)

	Modular	Finite difference
f_1'	115.12	—
f_2'	24.68	—
f_3'	160.20	—
$A'\theta_D$	107.50	—
$S'F_{aD}$	2.34	—
A	224.25	2245.40
S	4.91	176.76
Total	639.29	2422.16

Table 5 Transport wing design

	Initial design	Final design
Gross weight, N	4.391×10^5	4.150×10^5
Wing weight, N	2.779×10^4	1.728×10^4
Usable fuel weight, N	2.190×10^4	1.876×10^4
Range margin, %	17	1
Chord lengths, m		
Root	6.916	5.912
Break	3.765	3.218
Tip	1.725	1.234
Root to break, m	5.754	4.918
Break to tip, m	12.250	10.443
Sweep angle, deg	26.1	18.8
Ply orientation, deg	27.2	25.6

The structure is designed to withstand a 2.5g pull-up maneuver with a 1.5 factor of safety. The maneuver is assumed to follow an altitude loss and occurs at 2.5 times the cruise dynamic pressure. The wing skin is made of 0, ± 45, and 90-deg graphite-epoxy laminate with the zero direction being a design parameter used to create favorable bending-twist coupling so as to prevent aeroelastic divergence. Maximum strain constraints of 0.012 in the fiber and normal direction and in the shear were imposed on each ply. Spar caps are made of unidirectional material with a maximum stress capacity of 0.262 GPa. The structure was modeled by a finite element model shown in Fig. 1 and analyzed with a modification of the WIDOWAC program.[12] The wing was required to have an aeroelastic divergence dynamic pressure larger than 1.2 times the dynamic pressure at the pull-maneuver.

The aerodynamic design is primarily controlled by the requirement for the range to be equal to that of the reference aircraft (2340 km). The aerodynamic loads on wing were calculated using a vortex lattice model with 120 panels. The airfoil section used for all spanwise stations is a natural laminar flow airfoil designated as HSNLF(1)-0213, described in Ref. 15. The viscous drag is computed using section lift coefficients and a drag polar obtained from data in Ref. 15. The details of the calculation of the range are given in the Appendix. It is shown in the Appendix that for an airplane flying at optimal altitude the drag at cruise is proportional to the weight (this is not true if the altitude is fixed). The range of the aircraft is calculated by assuming that the drag at cruise is constant. That constant drag is calculated for a weight corresponding to half of the usable fuel.

Table 2 lists the design variables used for the optimization procedure. The first six variables are planform design variables shown in Fig. 2. The next two variables are twist angle variables that provide a rough definition of the jig shape of the wing. That is, the optimization procedure selects these variables so that the wing will deform into a good shape during cruise.

The two performance variables listed in Table 2 affect mostly the range. The cruise dynamic pressure is a surrogate for the cruise altitude and together with the usable fuel is selected so as to achieve the desired range at minimum weight.

There are 24 structural design variables that define the thickness of the 0-, 90-, and 45-deg plies. The wing is divided into four regions—two in the inboard box (see Fig. 1) and two in the outboard box. The line A-A in Fig. 1 marks the division of the inboard box and the line B-B marks the division of the outboard box. The ply thicknesses are taken to be constant in each region, making for 12 variables for the lower skin and 12 variables for the upper skin. Four design variables control the cross-sectional areas of the two front and two rear spar caps. Finally, one design variable is used to control the zero direction for the laminate for both lower and upper skins.

The constraints used in the optimization are listed in Table 3 and consist of the strain, stress, aeroelastic divergence, and range constraints discussed above. The last constraint is that the wing has enough volume for the fuel.

Approximate Optimization Procedure

The wing optimization can be formulated as

$$\begin{aligned} &\text{Minimize} && W(\boldsymbol{p}) \\ &\text{such that} && \boldsymbol{g}_s(\boldsymbol{p}) \geq 0 \\ &&& V_s(\boldsymbol{p}) \geq V_r \\ &&& R_c(\boldsymbol{p},D) \geq R_r \end{aligned} \tag{42}$$

where the vector $\boldsymbol{g}_s$ represents the structural constraints on the stresses, strains, and aeroelastic stability. The quantities V_s and V_r are the available wing volume and the required fuel volume, respectively. The calculated range R_c depends on the total drag of the aircraft and is required to be greater than the range of the reference aircraft.

To further reduce the computational cost, we use a sequential approximation optimization algorithm with move limits. The range constraint is calculated exactly from a linear approximation to the drag. Each approximate optimization problem starting from an initial design $\boldsymbol{p}^0$ is formulated as

$$\text{Minimize} \qquad W(\boldsymbol{p})$$

such that
$$g_s(p^0) + \sum_i^{n_v} \frac{\partial g_s}{\partial p_i} \Delta p_i \geq 0$$
$$V_s(p) \geq V_r$$
$$R_c(p,D) \geq R_r$$

where
$$D = D(p^0) + \sum_i^{n_v} \frac{\partial D}{\partial p_i} \Delta p_i \tag{43}$$

and n_v is the number of design variables.

The optimizer used is the NEWSUMT-A program,[16] which is based on an extended interior penalty function procedure and allows for various levels of constraint and objective function approximations.

Results and Discussion

The cost of sensitivity analysis using the modular approach is compared to the cost of calculating them by finite differences in Table 4. It is seen that the cost is reduced by a factor of 4. Additional savings are possible by calculating the individual disciplinary sensitivities f_1, f_2, and f_3 analytically instead of finite differences. However, this would require more familiarity with and access to the insides of the black-box packages.

The initial design selected for the optimization was similar to that obtained in Ref. 8, which resulted in gross aircraft weight of 439,100 N (98,700 lb) compared to 449,400 N (101,000 lb) for the reference aircraft. Using the sequential approximate optimization, the design process required seven iterations with the initial and final designs shown in Table 5. The gross weight convergence history is shown in Fig. 3. The gross weight of the aircraft was reduced to 415,000 N (93,280 lb). This 7.7% reduction in weight compared to the reference aircraft is partly due to the change in Mach number (0.78 for reference transport vs 0.48 for the design aircraft) and the accompanying drag reduction. The lower drag associated with the subsonic flight regime is responsible for the 17% excess range for the initial design. The reduced excess initial drag permitted a 3140 N (706 lb) reduction in fuel weight with an accompanying reduction in the size of the wing required for supplying enough lift for carrying the weight of the transport without excessive drag. Another source of weight savings was a reduction in the outboard portion of the wing from 52.3% of the total area of the wing to 50.8%. This shift of area can be expected to increase drag somewhat, but it has a larger effect on the bending moment on the structure. The reduction in structural weight accompanying the reduction in bending moment reduces the required lift and, therefore, ultimately reduces the drag.

Some insight into the working of the optimization process may be obtained by considering the design iterations to be divided into two stages. In the first stage, comprising the first four design cycles, the overall size of the wing and the fuel weight is reduced almost uniformly by 13–14%. This reflects the fact that for the lower cruise speed we may have a higher angle of attack and a smaller wing without incurring an excessive drag penalty. The second stage, comprising the last three design cycles, involves a substantial reduction in sweep, taper ratio, and further fuel reduction. This represents a finer refinement of the wing shape.

Concluding Remarks

The integrated aerodynamic-structural design of a subsonic transport wing for minimum weight subject to required range was formulated and solved. The problem requires large computational resources, and two methods were used to alleviate the computational burden. First a modular sensitivity method that permits the usage of black-box disciplinary software packages was used to reduce the cost of sensitivity derivatives. In particular, it was shown that derivatives of the aeroelastic response and divergence speed can be calculated without the costly computation of derivatives of aerodynamic influence coefficient and structural stiffness matrices. A sequential approximate optimization was used to further reduce computational cost. The optimization procedure was shown to require a small number of analysis and sensitivity calculations.

The design results presented in this paper should be considered representative of a multidisciplinary design of a transport wing with the present objective function and constants. Improved design results with this methodology including a more accurate structural-aerodynamic interface and landing speed constraints appear in Ref. 17.

Appendix: Range Calculation

If we neglect the small effect of changes in elastic deformation due to the change in weight, we can write the drag D of the aircraft as

$$D = qS_a C_D(C_L) \tag{A1}$$

where q is the dynamic pressure, S_a the wing area, and C_D the drag coefficient, which we assume to be a function of the cruise lift coefficient C_L. The lift coefficient may be written as

$$C_L = W/qS_a \tag{A2}$$

where W is the aircraft weight. To find the optimum dynamic pressure q_m (and, hence, the optimum altitude), we differentiate D with respect to q and set to zero whereby

$$S_a C_D - \frac{W}{q} \frac{\mathrm{d}C_D}{\mathrm{d}C_L} = 0 \tag{A3}$$

or

$$q_m = \frac{W}{S_a C_D} \frac{\mathrm{d}C_D}{\mathrm{d}C_L} \tag{A4}$$

Finally, Eq. (A1) is written for minimum drag D_m by using q_m and C_{L_m}, the corresponding optimum lift coefficient as

$$D_m = W \frac{\mathrm{d}C_D}{\mathrm{d}C_L}(C_{L_m}) \tag{A5}$$

which indicates that D_m is proportional to W. For an elastic wing, we assume that the minimum drag is still proportional to the weight, calculating the constant of proportionality, $\bar{D} = \mathrm{d}C_D/\mathrm{d}C_L$, at a weight W_0, corresponding to the half-fuel condition. We assume $\bar{D}$ to be approximately constant over the range

$$D_m = \bar{D}W \tag{A6}$$

The rate of change of aircraft weight due to fuel being consumed is

$$\frac{\mathrm{d}W}{\mathrm{d}t} = -c'T = -c'D = -c'\bar{D}W \tag{A7}$$

where c' is the thrust specific fuel consumption and T is the thrust. Integrating Eq. (A7) from an initial time t_i to a final time t_f, we get

$$\log(W_i/W_f) = c'\bar{D}(t_f - t_i) \tag{A8}$$

We assume that the aircraft is flying at a constant speed V_c, therefore, the cruise range R_c may be given as

$$R_c = V_c(t_f - t_i) = \frac{V_c}{c'\bar{D}} \log\left(\frac{W_i}{W_f}\right) \tag{A9}$$

The calculation of $\bar{D}$ requires a priori knowledge of the optimum dynamic pressure q_m. Instead of calculating q_m from Eq. (A4), we consider it to be a design variable, and its solution evolves with the other design variables through the integrated design process.

Acknowledgment

The Virginia Polytechnic Institute portion of this research was funded by the National Science Foundation under Grant DMC-8615336 and by the NASA Langley Research Center under Grant NAG-1-603. The authors would like to thank E. Unger of the Aerospace and Ocean Engineering Department for his assistance in some of the computational matters.

References

[1]Haftka, R. T., "Structural Optimization with Aeroelastic Constraints—A Survey of US Applications," *International Journal of Vehicle Design*, Vol. 7, 1986, pp. 381–392.

[2]Shirk, H. M., Hertz, T. Z., and Weisshaar, T. A., "A Survey of Aeroelastic Tailoring—Theory, Practice, and Promise," *Journal of Aircraft*, Vol. 23, No. 1, 1986, pp. 6–18.

[3]Grossman, B., Gürdal, Z., Strauch, G. J., Eppard, W. M., and Haftka, R. T., "Combined Aerodynamic/Structural Design of a Sailplane Wing," *Journal of Aircraft*, Vol. 25, No. 9, 1988, pp. 855–860.

[4]Wrenn, G. A., and Dovi, A. R., "Multilevel Decomposition Approach to the Preliminary Sizing of a Transport Aircraft Wing," *Journal of Aircraft*, Vol. 25, 1988, pp. 632–638.

[5]Sobieszczanski-Sobieski, J., "Multidisciplinary Optimization for Engineering Systems: Achievements and Potential," *Lecture Note in Engineering Series*, Vol. 47, Springer Verlag, Berlin, 1989, pp. 42–63; also published as NASA TM-101566.

[6]Livne, E., Schmit, L. A., and Friedmann, P., "An Integrated Approach to the Optimum Design of Actively Controller Composite Wings," AIAA Paper 89-1268, April 1989.

[7]Haftka, R. T., Grossman, B., Eppard, W. M., Kao, P. J., and Polen, D., "Efficient Optimization of Integrated Aerodynamic-Structural Design," *International Journal for Numerical Methods in Engineering*, Vol. 28, 1989, pp. 593–607.

[8]Shuart, M. J., Haftka, R. T., and Campbell, R. L., "Optimization Design of Swept-Forward High-Aspect-Ratio Graphite-Epoxy Wings," *Recent Advances in Multidisciplinary Analysis and Optimization*, edited by J-F. M. Barthelemy, NASA CP-3031, 1988, pp. 509–527.

[9]Sobieszczanski-Sobieski, J., "Sensitivity Analysis and Multidisciplinary Optimization for Aircraft Design: Recent Advances and Results," International Council of the Aeronautical Sciences, Paper 88-1.7.3, 1988.

[10]Sobieszczanski-Sobieski, J., "On the Sensitivity of Complex Internally Coupled Systems," *AIAA Journal*, Vol. 28, No. 1, 1990, pp. 153–160.

[11]Bertin, J. J., and Smith, M. L., *Aerodynamics for Engineers*, Prentice Hall, Englewood Cliffs, NJ, 1979, pp. 186–207.

[12]Haftka, R. T., and Starnes, J. H., Jr., "WIDOWAC: Wing Design Optimization with Aeroelastic Constraints—Program Manual," NASA TM X-3071, Oct. 1974.

[13]Rodden, W. P., "Aeroelastic Divergence of Unrestrained Vehicles," *Journal of Aircraft*, Vol. 21, No. 1, 1984, pp. 94–96.

[14]Rodden, W. P., "Comment on General Formulation of the Aeroelastic Divergence of Composite Swept-Forward Wing Structures," *Journal of Aircraft*, Vol. 26, No. 7, 1989, pp. 694–695.

[15]Sewall, W. G., McGhee, R. J., Viken, J. K., Waggoner, E. J., Walker, B. S., and Millard, B. F., "Wind-Tunnel Results for a High-Speed, Natural Laminar-Flow Airfoil Designed for General Aviation Aircraft," NASA TM-87602, 1987.

[16]Grandhi, R. V., Thareja, R., and Haftka, R. T., "NEWSUMT-A: A General Purpose Program for Constrained Optimization Using Constraint Approximations," *Journal of Mechanisms, Transmissions and Automation in Design*, Vol. 107, 1985, pp. 94–99.

[17]Unger, E. R., Rais-Rohani, M., Hutchinson, M. G., Haftka, R. T., and Grossman, B., "Multi-disciplinary Design of a Subsonic Transport Wing," *Proceedings of the Third Air Force/NASA Symposium on Recent Advances in Multidisciplinary Analysis and Optimization*, San Francisco, CA (to be published).